Effect of the Angle between Wind Stress and Wind Velocity Vectors on the Aerodynamic Drag Coefficient at the Air–Sea Interface

LE NGOC LY

Institute for Naval Oceanography, Stennis Space Center, Mississippi

16 July 1991 and 16 March 1992

ABSTRACT

It has long been accepted that wind stress and wind velocity vectors at the air–sea interface have the same direction. Observations show that there is an angle θ between these vectors, which in many cases can reach 20° or more. An equation for the mean energy flux related to the y components of stresses and velocities is developed. This equation is used with the other basic equations and boundary conditions for a coupled model, taking surface wave effects into account. Various numerical experiments are carried out using this coupled model to study the effect of the angle on aerodynamic drag coefficients. The numerical results show that θ angles of 10° and 20° tend to reduce the magnitudes of both drag coefficient and geostrophic drag coefficient between 10% and 20%, which agrees better with observations.

1. Introduction

Ly (1986, 1990) studied surface wave effects numerically by modeling energy transfer from the atmosphere to the ocean. He has suggested that a part of the energy from the atmosphere will generate and maintain surface gravity waves and another part will maintain drift current in the ocean. Based on conservation of energy through the surface wave layer and dimensional analysis, he wrote the equations for the turbulent kinetic energy flux and the mean energy flux. By using the traditional assumption that wind stress and wind velocity vectors at the air–sea interface have the same direction, and using the equation for the mean energy flux at the air–sea interface, he obtained a discontinuity boundary condition at the interface for the x component of velocity. The y component of velocity was assumed to be continuous across the interface. The traditional continuity boundary conditions for the momentum fluxes across the air–sea interface were used.

It has been traditionally assumed that the wind vector and wind stress vector are in the same direction, at least within the surface layer. Observations of Geernaert (1988, hereafter GG) over the North Sea and aircraft measurements by Zemba and Friehe (1987, hereafter ZF) over oceans showed that there is an angle (hereafter angle θ) between the wind vector and wind stress vector in the surface layer. The measurements were made for wind stress at 7.5 and 33 m (GG) and various heights (ZF) but not for surface wind stress. The observed angles between wind stress and wind velocity vectors have varied considerably. In all practical applications, the wind at 10-m height is generally accepted as the surface wind. Both GG and ZF showed that the angle θ strongly depends on height and the atmospheric stratification. Geernaert suggested regression equations for the angle θ dependent on both height and stratification. These studies (GG, ZF) demonstrated that in many cases this angle reaches 20° or more. In general, their studies showed that the wind velocity and stress vectors are rarely aligned. In this case, another equation for the mean energy flux related to the y component of stresses and velocities must be added to the basic model equations and boundary conditions for the coupled model, taking into account surface wave effects (see Ly 1986, 1990).

The aerodynamical drag coefficient depends on wind speed, near-surface atmospheric stratification, ocean surface waves, and other physical characteristics at the air–sea interface. The first two factors are best understood. Surface waves affect the drag coefficient, but the exact relationship is poorly known.

In this paper, we study numerically the effect of the angle between wind stress and wind vectors on the aerodynamic drag coefficient using a coupled model taking into account surface wind wave effects. Comparisons will also be made between numerical model results and available data on drag coefficients.

2. The generic equations

Friction velocity for airflow can be written in the general form as

$$u_*^2 = (\overline{u'w'}^2 + \overline{v'w'}^2)^{1/2}, \quad (1)$$

Corresponding author address: Dr. Le Ngoc Ly, Center for Ocean and Atmospheric Modeling, USM, Stennis Space Center, MS 39529.

where u', v', and w' are the fluctuating components in the x, y, and z directions, respectively. Traditionally, it has been assumed that the $\overline{v'w'}$ term is negligible with respect to the $\overline{u'w'}$ term. This means that the wind and stress vectors are aligned in the same direction, and the angle θ between the stress and wind vectors

$$\tan\theta = \overline{v'w'}/\overline{u'w'} \tag{2}$$

is zero. The positive angles correspond to the stress vector oriented to the right of the wind vector (Geernaert 1988).

Generalizing the problem, the friction velocity can be written in the form

$$u_* = (u_{*x}^4 + u_{*y}^4)^{1/4}, \tag{3}$$

where $u_{*x}^2 = -|\overline{u'w'}|$ and $u_{*y}^2 = -|\overline{v'w'}|$.

Ly (1986, 1990) gives the equations for the mean energy flux across the air–sea interface, based on conservation of energy through the wave layer and dimensional analysis, assuming $\theta = 0°$. In the more general case, for $\theta \neq 0°$, the equations for the mean energy flux across the air–sea interface have the forms:

$$(\rho_a\overline{u_a'w_a'})u_a|_{z_{0a}} + (\rho_s\overline{u_s'w_s'})u_s|_{z_{0s}} = C_1\rho_a u_{*ax}^3 \tag{4}$$

$$(\rho_a\overline{v_a'w_a'})v_a|_{z_{0a}} + (\rho_s\overline{v_s'w_s'})v_s|_{z_{0s}} = C_2\rho_a u_{*ay}^3, \tag{5}$$

where the subscript a refers to air and s refers to seawater. The roughness lengths at the upper and lower boundaries of the wave layer are z_{0a} and z_{0s}, the air and seawater densities are ρ_a and ρ_s, and the velocity components of both fluids are u and v. The nondimensional parameter C_1 (Ly 1986, 1990) and a companion C_2 represent the surface wind wave effect. The parameters C_1 and C_2 are not arbitrary constants but depend on directional wave spectra. Parameter C_2 represents an additional contribution of mean energy flux to the wave generation process. Here the relation between C_1u_{*x} and C_2u_{*y} is defined by $C_2u_{*y}/C_1u_{*x} = \tan\theta$, and by using Eq. (2) we have the following equation that defines θ for given C_1 and C_2.

$$(\tan\theta)^{1/2} = \frac{C_2}{C_1} = \frac{u_{*ay}}{u_{*ax}}. \tag{6}$$

The traditional continuity conditions across the air–sea interface for shear stress in the general case can be written in the form

$$(\rho_a u_{*ax}^2)|_{z_{0a}} = (\rho_s u_{*sx}^2)|_{s_{os}} \tag{7}$$

$$(\rho_a u_{*ay}^2)|_{z_{0a}} = (\rho_s u_{*sy}^2)|_{z_{os}}. \tag{8}$$

Using Eq. (1) for both fluids, Eqs. (4) and (5) can be written in the following forms:

$$\rho_a u_{*ax}^2 u_a|_{z_{0a}} + \rho_s u_{*sx}^2 u_s|_{z_{os}} = C_1\rho_a u_{*ax}^3 \tag{9}$$

$$\rho_a u_{*ay}^2 v_a|_{z_{0a}} + \rho_s u_{*sy}^2 v_s|_{z_{os}} = C_2\rho_a u_{*ay}^3. \tag{10}$$

By substituting Eqs. (7) and (8) into Eqs. (9) and (10), the following boundary conditions for velocities at the air–sea interface are

$$u_a(z_a)|_{z_{0a}} + u_s(z_s)|_{z_{0s}} = C_1u_{*ax} \tag{11}$$

$$v_a(z_a)|_{z_{0a}} + v_s(z_s)|_{z_{0s}} = C_2u_{*ay}. \tag{12}$$

These equations are nondimensionalized by setting

$$u_{ni} = (-1)^l(k/u_{*i})u_i; \quad v_{ni} = (-1)^l(k/u_{*i})v_i;$$

$$z_{ni} = fz_i/(ku_{*i}) = z_i/\Omega_i, \tag{13}$$

where $\Omega_i = ku_{*i}/f$ is the order of the planetary boundary-layer thickness. The von Kármán constant is taken to be $k = 0.4$. The Coriolis parameters is $f = 2\omega\sin\phi$ (ω is angular velocity of the earth's rotation and ϕ is latitude). The subscript n hereafter indicates any quantity in nondimensional form. Again the subscript $i = a$ represents the physical characteristics of airflow and $i = s$ represents those of seawater flow. The exponent in Eq. (13) $l = 1$ for the ocean and $l = 2$ for the atmosphere.

Inserting Eq. (13) into Eqs. (11) and (12), we have boundary conditions for the components of velocities:

$$u_{na}(z_{na})|_{z_{0na}} = -\left(\frac{\rho_a}{\rho_s}\right)^{1/2} u_{ns}(z_{ns})|_{z_{0ns}} + kC_1 \tag{14}$$

$$v_{na}(z_{na})|_{z_{0na}} = -\left(\frac{\rho_a}{\rho_s}\right)^{1/2} v_{ns}(z_{ns})|_{z_{0ns}} + kC_2. \tag{15}$$

It is noted from Eq. (6) that if $C_2 = 0$, wind stress and wind vectors have the same direction so that the angle $\theta = 0°$, and we have the situation described by Ly (1986, 1990).

3. The method of solution

The equations for nondimensional wind and drift current profiles can be written following Ly (1986). The wind profiles in the atmosphere are as follows:

$$u_{na} = \frac{k}{u_{*a}} U_{ga}\cos\alpha_a + \frac{d\sigma_{na}}{dz_{na}} \tag{16}$$

$$v_{na} = \frac{k}{u_{*a}} U_{ga}\sin\alpha_a - \frac{d\eta_{na}}{dz_{na}}. \tag{17}$$

The drift current profiles in the ocean are

$$u_{ns} = -\frac{k}{u_{*s}} U_{gs}\cos\alpha_s + \frac{d\sigma_{ns}}{dz_{ns}} \tag{18}$$

$$v_{ns} = -\frac{k}{u_{*s}} U_{gs}\sin\alpha_s - \frac{d\eta_{ns}}{dz_{ns}}, \tag{19}$$

where

$$U_{gi}\cos\alpha_i = -\frac{1}{f\rho_{0i}}\frac{\partial p_i}{\partial y_i}; \quad U_{gi}\sin\alpha_i = \frac{1}{f\rho_{0i}}\frac{\partial p_i}{\partial x_i} \tag{20}$$

are the geostrophic velocity components, and α_i are the angles between the surface wind and the geostrophic wind ($i = a$) and geostrophic current ($i = s$). The nondimensional vertical flux components of horizontal momentum in the x and y direction for both flows are η_{ni} and σ_{ni} (see Ly 1986).

Substituting Eqs. (16)–(19) into Eqs. (14) and (15), the formulas linking atmospheric and oceanic physical characteristics can be obtained:

$$\frac{k}{u_{*a}} U_{ga}\left[\cos\alpha_i + \frac{U_{gs}}{U_{ga}}\cos\alpha_s\right] = -\left[\frac{d\sigma_{na}}{dz_{na}} + \left(\frac{\rho_a}{\rho_s}\right)^{1/2}\frac{d\sigma_{ns}}{dz_{ns}}\right]\Bigg|^{z_{0na}} + kC_1 \quad (21)$$

$$\frac{k}{u_{*a}} U_{ga}\left[\sin\alpha_a + \frac{U_{gs}}{U_{ga}}\sin\alpha_s\right] = \left[\frac{d\eta_{na}}{dz_{na}} + \left(\frac{\rho_a}{\rho_s}\right)^{1/2}\frac{d\eta_{ns}}{dz_{ns}}\right]\Bigg|_{z_{0na}} + kC_2. \quad (22)$$

Using (21) and (22), it is easy to obtain expressions for the geostrophic drag coefficient (C_{Dg}) and angle (α_a) between the vectors of the surface wind and the geostrophic wind

$$C_{Dg}^2 = \left(\frac{u_{*a}}{kU_{ga}}\right)^2 = \frac{1 - 2m_0\cos\beta + m_0^2 + 2kC_{Dg}^2 N}{M_1^2 + M_2^2} + \frac{k^2 C_{Dg}^2 (C_1^2 + C_2^2)}{M_1^2 + M_2^2} \quad (23)$$

$$\tan\alpha_a = -\frac{1 - m_0(M_0\sin\beta + \cos\beta)}{M_0 - m_0(\cos\beta - M_0\sin\beta)} + \frac{kC_{Dg}(C_1 + C_2)}{\cos\alpha_a[M_0 - m_0(\cos\beta - M_0\sin\beta)]}, \quad (24)$$

where

$$m_0 = \frac{U_{gs}}{U_{ga}}; \quad \beta - 360° = \alpha_s - \alpha_a;$$

$$\left(\frac{\rho_a}{\rho_s}\right)^{1/2} \approx \frac{1}{28} \quad (25)$$

$$N = (C_1 M_1 + C_2 M_2) \quad (26)$$

$$M_1 = \left[\frac{d\eta_{na}}{dz_{na}} + \left(\frac{\rho_a}{\rho_s}\right)^{1/2}\frac{d\eta_{ns}}{dz_{ns}}\right]\Bigg|_{z_{0ni}} \quad (27)$$

$$M_2 = \left[\frac{d\sigma_{na}}{dz_{na}} + \left(\frac{\rho_a}{\rho_s}\right)^{1/2}\frac{d\sigma_{ns}}{dz_{ns}}\right]\Bigg|_{z_{0ni}} \quad (28)$$

$$M_0 = M_1/M_2 \quad (29)$$

and β is the angle between the geostrophic wind and geostrophic current. It is noted that the parameters C_1 and C_2, representing the surface wave and angle θ [Eq. (6)] effects are present in Eqs. (21)–(24) and, through these characteristics, affect the structure of the atmospheric and oceanic boundary layers. Equations (16)–(24), together with the complete model for air–sea interaction (see Ly 1986), are solved numerically by the pivotal condensation method (Ly 1989).

4. The numerical results and discussions

The aerodynamic drag coefficient C_D and geostrophic drag coefficient C_{Dg} are studied numerically by supposing the angle θ between stress and wind vectors is between 0° and 20°, which is defined by Eq. (6) through the given parameters C_1 and C_2. The parameter C_1 is taken equal to 4 (see Ly 1986) and C_2 varies between 0 and 2.41 to obtain θ between 0° and 20°. It is noted from Eq. (6) that the angle θ is always positive and is not dependent on the atmospheric stratification. Equation (6) also shows that θ depends on the ratio of two components of the friction velocity or the ratio of C_1 and C_2. This may suggest that both components of the friction velocity depend on the atmospheric stratification in the same way and the angle θ depends on the directional wave spectra. These problems need more theoretical and observational studies. The numerical results are shown in Figs. 1 and 2. Observational and model results of several published studies for the neutral drag coefficient (C_D) as a function of wind speed at 10-m height are shown in Fig. 1. It is noted that the differences between these drag coefficients are thought to be due to various sea states under which measurements were taken. Although there are large discrepancies between various curves, the drag coefficients of most authors [except curve 1 by Amorocho and DeVries (1981) and curve 7 by Large and Pond (1981)] increase with 10-m-height wind speed for the entire range of winds less than 10 m s^{-1}. As the wind speed increases above 10 m s^{-1}, these curves tend to diverge, and the drag coefficients vary greatly. Curves 10 and 11 in Fig. 1 are the model drag coefficients of this study for cases with $\theta = 0°$ and $\theta = 20°$, respectively. From this figure we can see that the model drag coefficient is very close to Hsu's (1986) result for wind less than 10 m s^{-1}. The drag coefficient increases nonlinearly over this wind interval. For winds greater than 15 m s^{-1}, drag coefficient C_D increases almost linearly and diverges from Hsu's. In the second case ($\theta = 20°$) (curve 11), the shape of the curve and values of the drag coefficients are very similar to those of Kondo (1975) for winds less than 25 m s^{-1}. Our model drag coefficient profile is shifted down from Kondo's profile at wind speeds less than 25 m s^{-1}. Comparing curves 10 and 11, we can see that magnitudes of C_D are less for the same wind speed in the second case. The drag coefficient obtained in the second case ($\theta = 20°$) is smaller than that in the first case ($\theta = 0°$) by 15% at wind speed 5 m s^{-1}, by 12% at 10 m s^{-1}, by

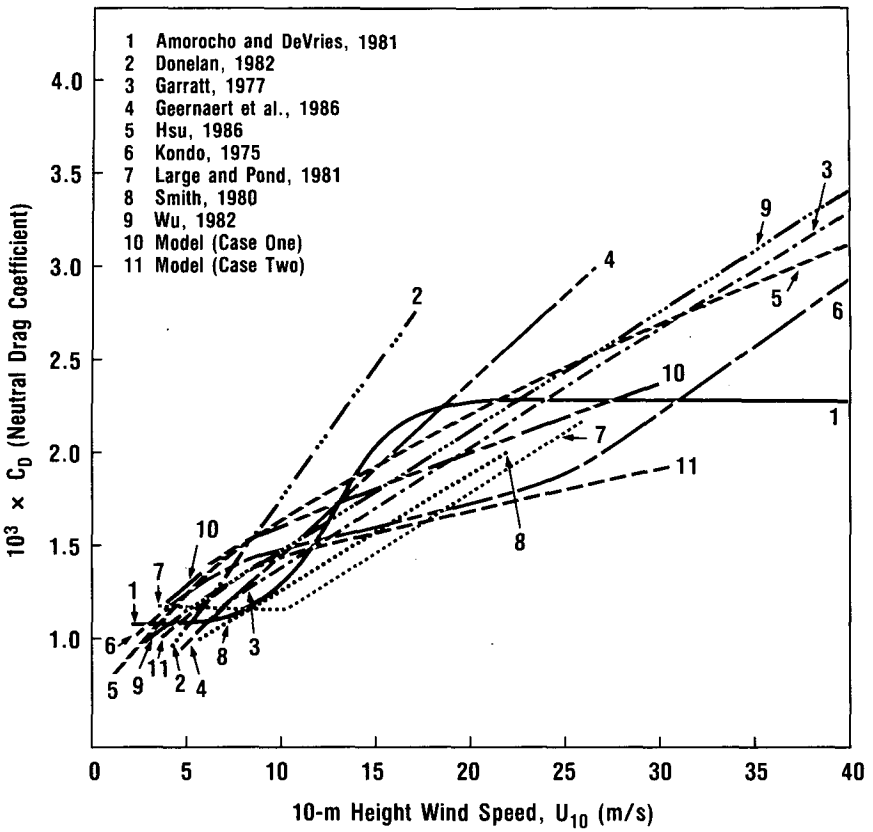

FIG. 1. The neutral drag coefficient, C_D, as a function of wind speed U_{10} at 10-m height. Curves 10 and 11 show the model drag coefficients for $\theta = 0°$ and $\theta = 20°$, respectively.

15% at 20 m s^{-1}, and by 20% for winds greater than 20 m s^{-1}. The computed drag coefficient for $\theta = 10°$ ($C_1 = 4$; $C_2 = 1.68$), which is not shown in Fig. 1, is smaller than that in the first case ($\theta = 0°$) by 11% at wind speed 5 m s^{-1}, by 12% at 10 m s^{-1}, by 15% at 30 m s^{-1}, and by 17% at 40 m s^{-1}. It is seen from the above comparisons of the drag coefficients that the existence of the angles θ between wind stress and wind vectors of 10° and 20° ($C_1 = 4$; $C_2 = 1.68$ and $C_1 = 4$; $C_2 = 2.41$) decreases the drag coefficients by 10%–20%. The effect is even more if the angle θ is greater (not shown here).

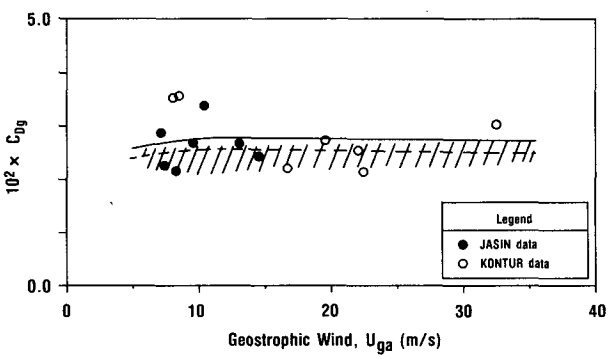

FIG. 2. The geostrophic drag coefficient, C_{Dg}, as a function of geostrophic wind speed (after Grant and Whiteford 1987). The shaded area shows their range of values of C_{Dg}. Solid and open circles are JASIN and KONTUR data, respectively. The model C_{Dg} is shown for $\theta = 0°$ (solid line) and $\theta = 20°$ (broken line), respectively.

Figure 2 shows the geostrophic drag coefficient (C_{Dg}) as a function of geostrophic wind speed (after Grant and Whiteford 1987). Their geostrophic drag coefficient is defined by $C_{Dg} = u_{*a}/U_{ga}$, which differs from the geostrophic drag coefficient in Eq. (23) by the von Kármán constant in the denominator. The shaded area in the figure shows the range of values of C_{Dg} obtained by Grant and Whiteford (1987) using data collected over the sea by an instrumented aircraft. The solid and open circles are JASIN and KONTUR data, respectively, collected during the 1978 JASIN experiment of the North Atlantic and the 1981 KONTUR experiment in the German Bight region in the North Sea (Grant and Whiteford 1978). Our model geostrophic drag coefficients are shown by the solid curve for the first case ($\theta = 0°$) and by the broken curve for the second case ($\theta = 20°$). We can see from the figure that in both cases the geostrophic drag coefficient is nearly independent of the geostrophic wind speed (except for

winds less than 10 m s^{-1}). The second curve is shifted down by almost 10% from the first curve. The average values are 2.8×10^{-2} for the first case and 2.5×10^{-2} for the second case. From Fig. 2, we can also see that the second case curve fits better with the data of JASIN and KONTUR and with Grant and Whiteford.

5. Remarks and conclusions

Wind stress and wind velocity vectors have long been assumed to have the same direction. Observations show that there is an angle between wind stress and wind velocity vectors, which in many cases reaches 20° or more. In the general case, an equation for the mean energy flux related to y components of stresses and velocities was added to the basic model equations and boundary conditions for a coupled model. Surface wave effects were taken into account to study the effect of the angle between wind stress and wind velocity vectors on the aerodynamic drag coefficient. Numerical experiments were carried out with given wave parameters $C_1 = 4$ and C_2 between 0 and 2.41 (θ between 0° and 20°). The numerical results show that for the parameters $C_1 = 4$ and $C_2 = 0$ ($\theta = 0°$), the model neutral drag coefficient is very close to Hsu's (1986) result for winds less than 10 m s^{-1}. The model drag coefficient for $C_1 = 4$ and $C_2 = 2.41$ ($\theta = 20°$) is very close to Kondo's (1975) result for winds less than 25 m s^{-1}. The existence of the angles between stress and wind vectors for $\theta = 10°$ and 20° tends to reduce the magnitudes of the aerodynamic drag coefficients by 10%–20% for winds less than 30 m s^{-1}. The effect is even larger for greater values of θ.

The model geostrophic drag coefficients, C_{Dg}, are almost independent of the geostrophic wind speed (except for winds less than 10 m s^{-1}). The angle $\theta = 20°$ reduces the magnitude of the geostrophic drag coefficient by about 10% to better fit the observations.

It is noted from Eq. (6) that the effect of angle θ at the air–sea interface is the effect of the y component of the surface momentum flux. This affects air–sea interaction parameters and atmospheric and oceanic physical characteristics such as boundary-layer depth, drift currents, etc., through (21) and (22), which link the physical characteristics of both fluids. This "angle" effect problem needs more theoretical and experimental studies, especially to determine the dependence of angle θ on height and stratification.

Acknowledgments. The author acknowledges Professor George L. Mellor at the Atmospheric and Oceanic Science Program, Princeton University, for discussions that generated the ideas of this research. This paper is a contribution to the project "Dynamics of Coupled Models," which is a component of the Naval Research Laboratory (NRL) Air–Sea Interaction Task. The author gratefully acknowledges Drs. J. Dana Thompson and John C. Kindle of NRL for their encouragement. The comments of two anonymous reviewers were very helpful. The author acknowledges the support of the Institute for Naval Oceanography (INO), which is an integral part of the NRL and is managed by the University Corporation for Atmospheric Research (UCAR).

REFERENCES

Amorocho, J., and J. J. DeVries, 1981: Reply. *J. Geophys. Res.*, **86**, 4308.

Donelan, M. A., 1982: The dependence of aerodynamic drag coefficient on wave parameters. *Proc. First Int. Conf. on Meteorology and Coast Zone*, Boston, Amer. Meteor. Soc., 381–387.

Garratt, J. R., 1977: Review of drag coefficients over oceans and continents. *Mon. Wea. Rev.*, **105**, 915–929.

Geernart, G. L., 1988: Measurements of the angle between the wind vector and wind stress vector in the surface layer over the North Sea. *J. Geophys. Res.*, **93**, 8215–8220.

——, K. Katsaros, and K. Richer, 1986: Variation of the drag coefficient and its dependence on sea state. *J. Geophys. Res.*, **91**, 7667–7679.

Grant, A. L. M., and R. Whiteford, 1987: Aircraft estimates of the geostrophic drag coefficient and Rossby similarity function *A* and *B* over the sea. *Bound.-Layer Meteor.*, **39**, 219–231.

Hsu, S. A., 1986: A mechanism for the increase of wind stress (drag) coefficient with wind speed over water surface: A parametric mode. *J. Phys. Oceanogr.*, **16**, 144–150.

Kondo, J., 1975: Air-sea bulk transfer coefficients in diabatic conditions. *Bound.-Layer Meteor.*, **9**, 91–112.

Large, W. G., and S. Pond, 1981: Open ocean momentum flux measurements in moderate to strong winds. *J. Phys. Oceanogr.*, **11**, 324–336.

Ly, L. N., 1986: Modeling the interaction between the atmospheric and oceanic boundary layers, including a surface wave layer. *J. Phys. Oceanogr.*, **8**, 1430–1443.

——, 1989: An application of the Pivotal-Condensation method to modeling the air–sea boundary-layer structure. *Math. Comput. Modelling*, **12**(9), 1117–1130.

——, 1990: Numerical studies of the surface wave effects on the upper turbulent layer in the ocean. *Tellus*, **42A**, 557–567.

Wu, J., 1982: Wind-stress coefficients over sea surface from breeze to hurricane. *J. Geophys. Res.*, **87**, 9704–9706.

Zemba, J., and C. A. Friehe, 1987: The marine atmospheric boundary layer jet in the Coastal Ocean Dynamics Experiment. *J. Geophys. Res.*, **92**, 1489–1496.